Journal of Power Sources 189 (2009) 1179–1183

Contents lists available at ScienceDirect

Journal of Power Sources

journal homepage: www.elsevier.com/locate/jpowsour

Short communication

Investigation of discharge reaction mechanism of lithium|liquid electrolyte|sulfur battery

Ho Suk Ryu[a,c], Zaiping Guo[a,b,*], Hyo Jun Ahn[c], Gyu Bong Cho[c], Huakun Liu[a,b]

[a] Institute for Superconducting and Electronic Materials, University of Wollongong, Wollongong, NSW 2522, Australia
[b] School of Mechanical, Materials & Mechatronic Engineering, University of Wollongong, Wollongong, NSW 2522, Australia
[c] Information Technology Research Center for Energy Storage and Conversion & i-cube Center, Gyeongsang National University, Jinju, 660-701, Republic of Korea

ARTICLE INFO

Article history:
Received 23 October 2008
Received in revised form 3 December 2008
Accepted 8 December 2008
Available online 27 December 2008

Keywords:
Lithium battery
Current density
Sulfur electrode
Discharge capacity

ABSTRACT

The influence of current density on the discharge reaction of Li–S batteries is investigated by discharge tests (first discharge curve), differential scanning calorimetry (DSC), X-ray diffraction (XRD) (discharge products), and scanning electron microscopy (the surface morphology of sulfur electrodes). The first discharge capacity and the plateau potential both decrease with increasing current density. When the current density is increased from 100 to 1600 mA g^{-1} S, the discharge capacity decreases from 1178 to 217 mAh g^{-1} S.

When the Li–S battery is discharged at low current density, i.e., below 400 mA g^{-1} S, elemental sulfur is fully converted to Li_2S, which is observable from XRD and DSC data. Only one plateau is observed in the discharge curve for current densities above 400 mA g^{-1} S. Part of the elemental sulfur still remains after discharging at high current densities (over 800 mA g^{-1} S). Thus the discharge capacity at high current density is smaller than that at low current density due to un-reacted elemental sulfur after discharge.

1. Introduction

There has been an increasing demand for batteries with high specific power and energy for applications in hybrid electric vehicles (HEVs), as well as other electrical devices. Sulfur is a very attractive positive electrode (cathode) material for lithium batteries due to its cheapness and high theoretical specific capacity. The Li–S battery has a high theoretical specific energy of 2600 W h kg^{-1}, which is much higher than those of commercial lithium-ion batteries [1–3].

Many researchers have published studies of the electrochemical properties of the Li–S cell, such as discharge capacity [1–15], cycling [5–8,11], and self-discharge [9] at room temperature. One of the most important factors is rate capability, because of the demands of HEVs and high-power electronic equipment [16,6].

Since sulfur is an electrically insulating material (5×10^{-30} S cm^{-1} at 25 °C), it is necessary to put conducting additives into the sulfur electrode. The insulating properties of the sulfur also make it very difficult to obtain high-rate capability. There have been several reports that the discharge capacity of Li–S batteries decreases with increasing current density [9,17–19]. Therefore, some researchers have investigated improving the rate capability by changing the composition of the sulfur electrode or the conducting additive. Cheon et al. [10] reported that a thicker sulfur electrode showed lower utilization. Also, they reported that the sulfur electrode was covered by a dense film, which could induce the decrease in capacity with current density because it would tend to block ionic transport towards the inside of the cathode. It was not possible, however, to identify clearly the dense film.

In order to improve the rate capability of the Li–S battery, it is very important to understand the discharge reaction mechanism at the various current densities. In this investigation, changes in the first discharge curves of Li–S batteries are investigated for various current densities. After discharge, the sulfur electrode is examined by structural and morphological analysis techniques, including X-ray diffraction (XRD), differential scanning calorimetry (DSC), and scanning electron microscopy (SEM). From the above results, the discharge mechanism is examined at different discharge current densities.

2. Experimental details

The sulfur cathode was prepared by coating a mixed slurry of sulfur, polyethylene oxide (PEO) and acetylene black (AB) carbon on an aluminum current-collector. The cathode consisted of 70 wt.% of elemental sulfur, 15 wt.% of PEO, and 15 wt.% of AB. The thickness

* Corresponding author at: Institute for Superconducting and Electronic Materials, University of Wollongong, Wollongong, NSW 2522, Australia.
Tel.: +61 2 4221 5225; fax: +61 2 4221 5731.
E-mail address: zguo@uow.edu.au (Z. Guo).

0378-7753/$ – see front matter © 2008 Elsevier B.V. All rights reserved.
doi:10.1016/j.jpowsour.2008.12.073

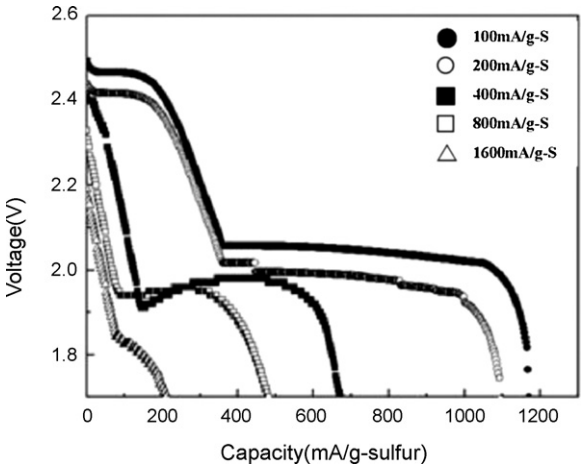

Fig. 1. First discharge profiles of Li–S batteries discharged at various current densities. Discharge of battery at 20 °C and cut-off at 1.7 V.

of the cathode layer was about 40 μm. The electrolyte consisted of 0.5 M lithium trifluoromethane sulfonate ($LiCF_3SO_3$) dissolved in tetraethylene glycol dimethylether (TEGDME). The anode was a lithium foil (thickness 380 μm, Cyprus Foote Mineral, USA). The electrode and electrolyte were prepared in a glove box purged with argon. The Li–S battery was assembled by stacking in turn the sulfur cathode, the porous polypropylene separator (Celgard 2200) soaked with electrolyte and the lithium anode. The cells were packaged to make Swagelok-type cells and assembled in an argon-filled glove-box. The cells were discharged to 1.7 V (vs. Li^+/Li) at various current densities from 100 to 1600 mA g^{-1} S.

The crystal structure of the sulfur electrode was investigated with an X-ray diffractometer at a scanning rate of 2° min^{-1} and Cu Kα radiation. The thermal stability of the sulfur electrode was evaluated with a differential scanning calorimeter at a heating rate of 2 °C min^{-1} from 100 to 120 °C. The surface morphology of the sulfur cathode was observed with a scanning electron microscope. In order to prevent contamination, all specimens were prepared in a glove-box purged with argon.

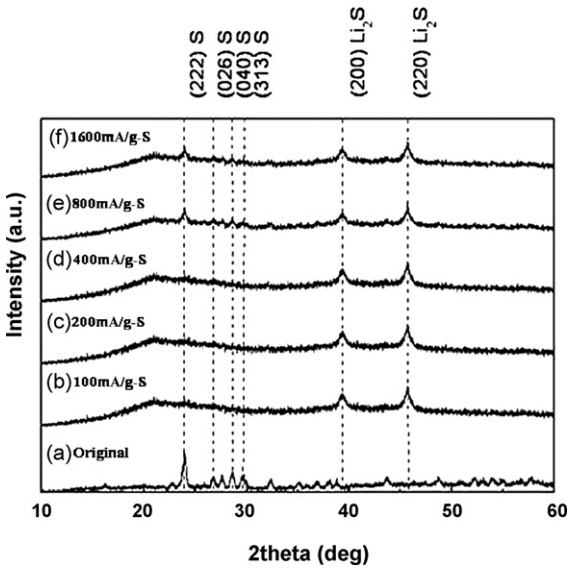

Fig. 2. XRD patterns of 70 wt.%-S electrodes discharged at (b) 100 mA g^{-1} S, (c) 200 mA g^{-1} S, (d) 400 mA g^{-1} S, (e) 800 mA g^{-1} S and (f) 1600 mA g^{-1} S. XRD pattern of initial electrode before discharge is presented in (a) for comparison.

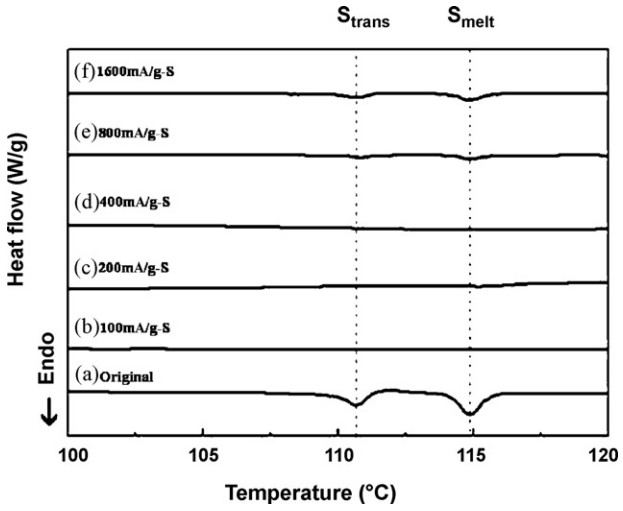

Fig. 3. DSC curves of 70 wt.%-S electrodes discharged at (b) 100 mA g^{-1} S, (c) 200 mA g^{-1} S, (d) 400 mA g^{-1} S, (e) 800 mA g^{-1} S and (f) 1600 mA g^{-1} S. Profile of initial electrode before discharge is presented for comparison in (a).

3. Results and discussion

Fig. 1 shows the first discharge curves of Li–S batteries discharged at various current densities from 100 to 1600 mA g^{-1} S. Discharge at 100 mA g^{-1} S, shows an upper plateau of 2.5 V and a lower plateau of 2.0 V. The upper plateau disappears when the battery is discharged at high current densities above 400 mA g^{-1} S. At 100 mA g^{-1}, the first discharge capacity is 1178 mAh g^{-1} S, which is 70% of the theoretical value (1675 mAh g^{-1} S), assuming complete reaction to the final product, Li_2S. When the current density is increased, the capacity continuously decreases to 217 mAh g^{-1} S for a current density of 1600 mA g^{-1} S.

The plateau potential and discharge capacity decrease with increasing current density. This result was similar to that previously reported [10]. It is well known that the internal resistance and the polarization of the electrode increase during discharge with increasing current density. The discharge reaction of the Li–S batteries investigated here may, however, change at different current densities because the shape of the discharge curves varies significantly with current density.

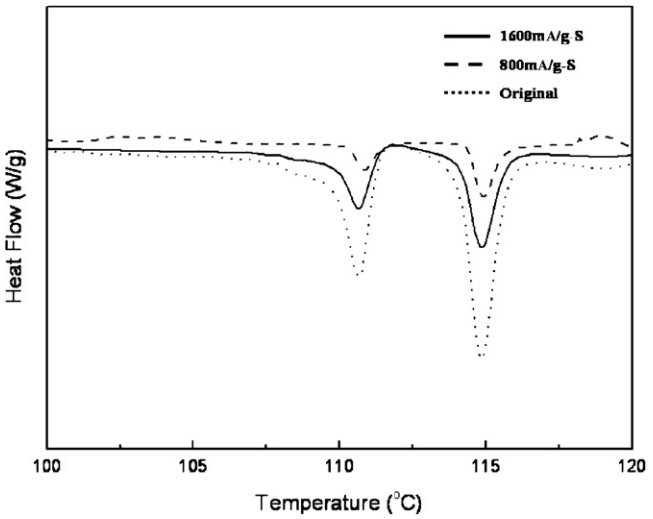

Fig. 4. DSC curves (temperature = 100–120 °C) of 70 wt.%-S electrodes before discharge and discharged at different current densities.

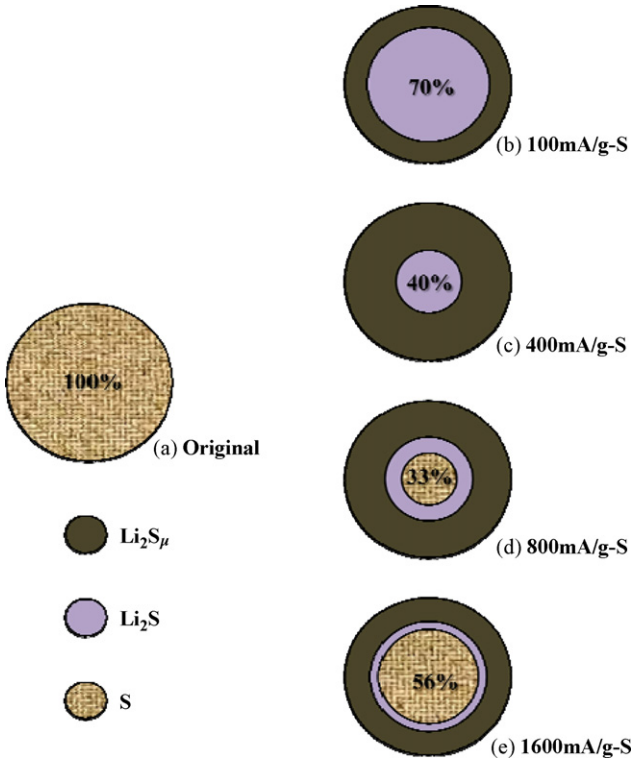

Fig. 5. Schematic diagram of ratios of materials in sulfur electrode discharged with various current densities by results of DSC, XRD, and discharge capacity measurements: (a) original, (b) 100 mA g^{-1} S, (c) 400 mA g^{-1} S, (d) 800 mA g^{-1} S and (e) 1600 mA g^{-1} S.

It is proposed that the discharge behaviour of a Li–S battery at low current density (100 mA g^{-1} S) corresponds to Eq. (1) for the upper plateau region and to Eq. (2) for the lower plateau region [19], i.e.:

$$Li_2 + nS \rightarrow Li_2S_n (n > 4) \quad (1)$$

$$2(n-1)Li + Li_2S_n \rightarrow nLi_2S \quad (2)$$

The elemental sulfur in the sulfur electrode was converted into Li_2S within two plateau potential regions when it was discharged at low current density. However, the discharge reaction at high current density might be different, as the upper plateau region was not visible at all when the Li–S battery was discharged at high current densities above 400 mA g^{-1} S.

In order to investigate the change in the discharge reaction with increasing current density, the sulfur electrodes were analyzed after discharging by using XRD, DSC, and SEM.

The XRD patterns of sulfur electrodes which were discharged at various current densities are shown in Fig. 2. The XRD pattern of the original sulfur electrode (a) without discharge was also shown in Fig. 2 for comparison purposes [19]. For the sulfur electrode which was discharged at the low current density of 100 mA g^{-1} S (Fig. 2(b)), we could not find any traces of sulfur peaks, and new peaks which correspond to Li_2S could be observed, which corresponds to the final product of Eqs. (1) and (2). No extra peaks, except those related to Li_2S, could be observed when the current density increases to 400 mA g^{-1} S (Fig. 2(b)–(d)). However, sulfur peaks as well as Li_2S peaks were observed in the sulfur electrodes which were discharged at high current density over 800 mA g^{-1} S (Fig. 2(e) and (f)). It was certain that the final product in all Li–S batteries is Li_2S, as reported in previous work [10,19].

After discharging at current densities its above 800 mA g^{-1} S, elemental sulfur still remains in the sulfur electrode, which means that part of the sulfur has not participated in the reaction during discharge at such current densities.

The proportion of sulfur remaining in the electrode after discharge was analyzed by DSC; profiles of the sulfur electrodes discharged at various current densities are shown in Fig. 3. The original sulfur electrode (Fig. 3(a)) gives two endothermic peaks at 111 and 115 °C, which result from elemental sulfur [19]. The two peaks disappear after the cell is discharged at a current density below 400 mA g^{-1} S, due to the absence of elemental sulfur. At high current density, i.e., over 800 mA g^{-1} S, peaks related to elemental sulfur are observed and thus confirm the existence of this mate-

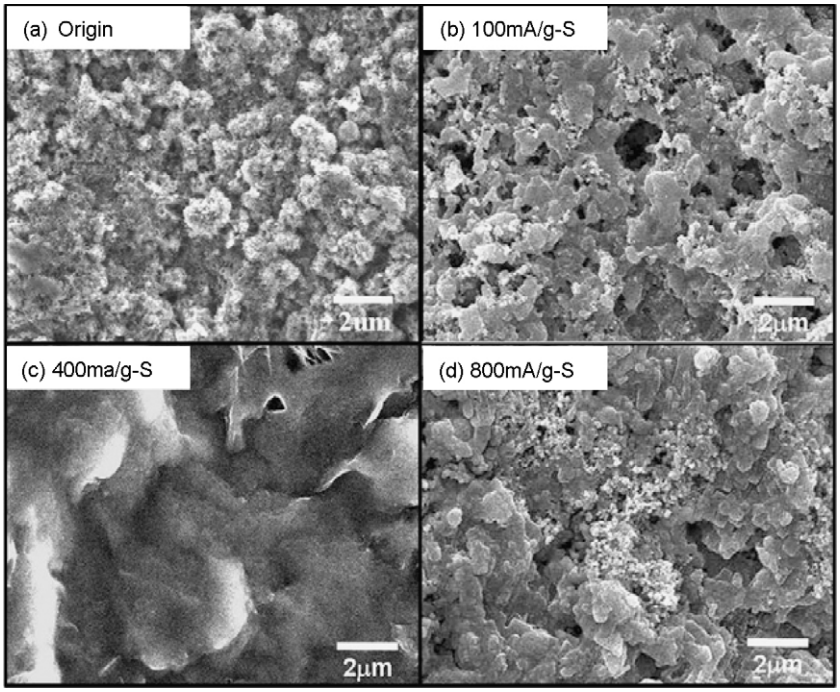

Fig. 6. SEM images of 70 wt.%-S electrode discharged at a current density of (a) original, (b) 100 mA g^{-1} S, (c) 400 mA g^{-1} S and (d) 800 mA g^{-1} S. Samples prepared by removing electrode from battery and then drying in glove-box purged with argon.

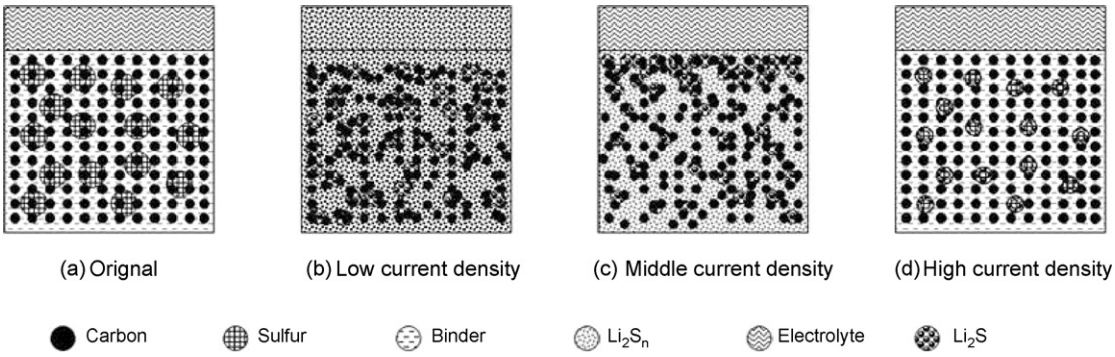

Fig. 7. Schematic diagram of morphology of sulfur electrode discharged at various current densities from results of DSC, XRD and discharge capacity measurements: (a) original, (b) low current density, (c) middle current density and (d) high current density.

rial in the electrode. The result is consistent with the XRD results presented above.

The sulfur peak area in the DSC curves increases with current density. The area of the DSC peaks corresponds to the heat of the reaction, which is related to the amount of sulfur. In order to calculate the amount of elemental sulfur remaining in the sulfur electrode after discharge at different current densities over 800 mA g^{-1} S, the area of the 115 °C peak, which resulted from the melting of the sulfur, was analyzed. The original sulfur electrode (Fig. 4(a)) shows a heat of fusion of 1.66 kJ mol^{-1}, which is almost identical to the theoretical heat of fusion of elemental sulfur, 1.71 kJ mol^{-1}. Comparison of the peak area at 115 °C of the discharged electrodes with that of the original electrode allows calculation of the proportion of sulfur remaining in the discharged electrodes. The fraction of sulfur in electrodes discharged at 800 and 1600 mA g^{-1} S is 33 and 56%, respectively.

Given that 56% of the elemental sulfur remains in the discharged electrode at 1600 mA g^{-1} S, the utilization of the sulfur electrode is 44% and, therefore, the discharge capacity should be 737 mAh g^{-1} S based on the theoretical value of 1675 mAh g^{-1} S. In fact, the first discharge capacity at 1600 mA g^{-1} S is 217 mAh g^{-1} S, which is only 13% of the theoretical amount. A possible explanation is that the intermediate product (lithium polysulfide) may still exist during the discharge reaction. The surfaces of the sulfur particles react with lithium and form Li_2S_n during the initial stage of discharge, and then Li_2S_n is converted to Li_2S during further discharge. The Li_2S has a low electronic conductivity and thereby restricts any reaction with the sulfur inside particles at high current density.

From the results of DSC, XRD and discharge capacity measurements, schematic diagrams of the ratios of sulfur, lithium polysulfide and Li_2S in a sulfur particle after discharge at various current densities have been constructed and are shown in Fig. 5.

For electrodes discharged at low current densities, elemental sulfur (100%, Fig. 5(a)) in the cathode is totally converted to Li_2S_n at the first plateau. The Li_2S_n then dissolves in the electrolyte and 70% (Fig. 5(b)) and 40% (Fig. 5(c)) is transformed to Li_2S at the second discharge plateau at 100 and 400 mA g^{-1}-S, respectively.

At high current densities (800 and 1600 mA g^{-1} S), elemental sulfur in the sulfur electrode is only partly changed to Li_2S_n, which is then partially converted to the final product, Li_2S, via a rapid reaction. For discharge at 800 mA g^{-1} S, 67% of the elemental sulfur is changed to Li_2S_n and 30% of this is transformed to Li_2S (Fig. 5(d)). At 1600 mA g^{-1} S, 44% of the elemental sulfur is changed to Li_2S_n, and then 12.5% of this is rapidly changed to Li_2S (Fig. 5(e)). This phenomenon is likely to be related to the reaction time, the electrical conductivity of the reactants, and the extent of Li ion transfer in the cathode.

Scanning electron micrographs of sulfur electrodes after discharge at various current densities are presented in Fig. 6. Particles in the electrode are gradually agglomerated as the current density increases, and a dense film is formed when the discharge current density is as high as 400 mA g^{-1} S. By contrast, further increase in current density to 800 mA g^{-1} S creates an electrode surface quite similar to that of the electrode discharged at 100 mA g^{-1} S. It is conducted that the surface features of the sulfur electrode are dependent on the rate of reaction, i.e., the current density.

At low current density (100 mA g^{-1} S), all elemental sulfur in the sulfur electrode is changed to Li_2S_n during the initial stage of discharge, and the Li_2S_n then dissolves in the electrolyte. The dissolved Li_2S_n will then move among the particles and be converted to Li_2S on the surface of the carbon (added to improve the conductivity of the cathode) (Fig. 7(b)). At medium current density (400 mA g^{-1} S), elemental sulfur is also converted to Li_2S_n and dissolves in the electrolyte during the initial discharge. The dissolved Li_2S_n cannot, however, be removed from the electrode, but accumulates on the surface of the electrode where it is converted to Li_2S to give the electrode a smooth appearance, as shown in the SEM image (Fig. 7(c)).

At high current density (above 800 mA g^{-1} S), the majority of the Li_2S_n may not dissolve in the electrolyte, but is converted to Li_2S on the surface of the sulfur particles and thereby restricts the reaction of the elemental sulfur inside the particles. The shape of the particles remains the same (Fig. 7(d)). Therefore, the SEM image of the sulfur electrode after discharge at high current densities is similar to that of the as-prepared electrode.

4. Conclusions

The discharge reaction of Li–S batteries at different current densities has been investigated by discharge tests, XRD, DSC, and SEM. With increasing current density, both the discharge capacity and the plateau voltage decrease. At low current density, discharged sulfur electrodes display only Li_2S peaks in XRD patterns. At high current density, however, both elemental sulfur and Li_2S, peaks are observed. Discharge capacities of the sulfur electrode greatly decrease after discharge at high current density (over 800 mA g^{-1} S) due to under-utilization of the active material.

Acknowledgements

Financial support from the Australian Research Council through Linkage Project LP0775456 is gratefully acknowledged. The authors also would like to thank Dr. Tania Silver at the University of Wollongong for critical reading of the manuscript.

References

[1] E.J. Cairns, E.C. Gay, R.K. Steunenberg, H. Shimotake, J.R. Selman, T.L. Wilson, D.S. Webster, Argonne Natl. Lab. Rep. (1972) 7953.
[2] E. Peled, A. Gorenshtein, M. Segal, Y. Sternberg, J. Power Sources 26 (1989) 269.

[3] D. Marmorstein, T.H. Yu, K.A. Striebel, F.R. McLarnon, J. Hou, E.J. Cairns, J. Power Sources 89 (2000) 219.
[4] J.H. Shin, S.S. Jung, K.W. Kim, H.J. Ahn, J.H. Ahn, J. Mater. Sci. 13 (2002) 723.
[5] Y.M. Lee, N.S. Choi, J.H. Park, J.K. Park, J. Power Sources 119–121 (2003) 964.
[6] S.C. Han, M.S. Song, H. Lee, H.S. Kim, H.J. Ahn, J.Y. Lee, J. Electochem. Soc. 150 (2003) A889.
[7] J.P. Shim, K.A. Striebel, E.J. Cairns, J. Electrochem. Soc. 149 (2002) A1321.
[8] H.S. Ryu, H.J. Ahn, K.W. Kim, J.H. Ahn, J.Y. Lee, E.J. Cairns, J. Power Sources 140 (2005) 365.
[9] S.E. Cheon, K.S. Ko, J.H. Cho, S.W. Kim, E.Y. Chin, H.T. Kim, J. Electrochem. Soc. 150 (2003) A796.
[10] S.E. Cheon, K.S. Ko, J.H. Cho, S.W. Kim, E.Y. Chin, H.T. Kim, J. Electrochem. Soc. 150 (2003) A800.
[11] D.R. Chang, S.H. Lee, S.W. Kim, H.T. Kim, J. Power Sources 112 (2002) 452.
[12] J. Wang, Y. Wang, X. He, J. Ren, C. Jiang, C. Wan, J. Power Sources 138 (2004) 271.
[13] J. Wang, L. Liu, Z. Ling, J. Yang, C. Wan, C. Jiang, Electrochim. Acta 48 (2003) 1861.
[14] S. Tobishima, H. Yamamoto, M. Matsuda, Electrochim. Acta 42 (1997) 1019.
[15] S. Kim, Y.J. Jung, S.J. Park, J. Power Sources 152 (2005) 272.
[16] Y.V. Mikhaylik, J.R. Akridge, J. Electochem. Soc. 150 (2003) A306.
[17] M.S. Song, S.C. Han, H.S. Kim, J.H. Kim, K.T. Kim, Y.M. Kang, H.J. Ahn, S.X. Don, J.Y. Lee, J. Electochem. Soc. 151 (2004) A791.
[18] B.H. Jeon, J.H. Yeon, K.M. Kim, I.J. Chun, J. Power Sources 109 (2005) 89.
[19] H.S. Ryu, H.J. Ahn, K.W. Kim, J.H. Ahn, J.Y. Lee, J. Power Sources 153 (2006) 360.